LMI final project - 4×4 ray matrix formalism

Gal Feldman[1] and Yuval Sever[1]

[1] *Raymond and Beverly Sackler School of Physics and Astronomy, Tel - Aviv University, Tel - Aviv 69978, Israel*

(Dated: May 25, 2024)

In this paper we will derive, and numerically validate the 4X4 ray pulse matrix formalism (Kostenbauder matrices) [1]. this formalism is an expansion of the known 2x2 ABCD matrix formalism for paraxial optical systems with disspersive elements. This expansion adds to the ray vector two more component, time and frequency, which allows to calculate (or simulate) more advanced optical systems in which the light frequency and phase matters to us. in this paper we will numerically simulate the various examples given in the original paper, and we will simulate a light beam passing through a pulse shaper. For the extra use case we will simulate a light beam passing through a monochromator.

I. INTRODUCTION

The 2X2 ray matrix formalism was first introduced by Kogelnik and Li in 1966 [2]. They presented it conventionally in the form :

$$\begin{bmatrix} x \\ \theta \end{bmatrix}_{out} = \begin{bmatrix} A & B \\ C & D \end{bmatrix} \begin{bmatrix} x \\ \theta \end{bmatrix}_{in} \tag{1}$$

where the vectors represent the perpendicular position and angle of the light beam before and after passing through the optical element. The ABCD matrix represents the optical element. The elements of the matrix is given by :

$$\begin{bmatrix} A & B \\ C & D \end{bmatrix} = \begin{bmatrix} \frac{\partial x_{out}}{\partial x_{in}} & \frac{\partial x_{out}}{\partial \theta_{in}} \\ \frac{\partial \theta_{out}}{\partial x_{in}} & \frac{\partial \theta_{out}}{\partial \theta_{in}} \end{bmatrix} \tag{2}$$

In the paper we chose, Kostenbauder expanded this formalism, by building on the work of O.E Martinez [3][4], he presented this convention :

$$\begin{bmatrix} x \\ \theta \\ t \\ f \end{bmatrix}_{\text{out}} = \begin{bmatrix} A & B & 0 & E \\ C & D & 0 & F \\ G & H & 1 & I \\ 0 & 0 & 0 & 1 \end{bmatrix} \begin{bmatrix} x \\ \theta \\ t \\ f \end{bmatrix}_{\text{in}} \tag{3}$$

Where :

$$\begin{bmatrix} A & B & 0 & E \\ C & D & 0 & F \\ G & H & 1 & I \\ 0 & 0 & 0 & 1 \end{bmatrix} = \begin{bmatrix} \frac{\partial x_{out}}{\partial x_{in}} & \frac{\partial x_{out}}{\partial \theta_{in}} & \frac{\partial x_{out}}{\partial t_{in}} & \frac{\partial x_{out}}{\partial f_{in}} \\ \frac{\partial \theta_{out}}{\partial x_{in}} & \frac{\partial \theta_{out}}{\partial \theta_{in}} & \frac{\partial \theta_{out}}{\partial t_{in}} & \frac{\partial \theta_{out}}{\partial f_{in}} \\ \frac{\partial t_{out}}{\partial x_{in}} & \frac{\partial t_{out}}{\partial \theta_{in}} & \frac{\partial t_{out}}{\partial t_{in}} & \frac{\partial t_{out}}{\partial f_{in}} \\ \frac{\partial f_{out}}{\partial x_{in}} & \frac{\partial f_{out}}{\partial \theta_{in}} & \frac{\partial f_{out}}{\partial t_{in}} & \frac{\partial f_{out}}{\partial f_{in}} \end{bmatrix} \tag{4}$$

As one can see, the new expanded formalism takes into consideration also the time and frequency components. By that, it allows a rational treatment for more complex optical configurations, specifically ones with spacial or temporal dispersion.

The definition in Eq (4) can be easily derived in a few steps. Firstly, looking at the upper left 2X2 block of the matrix, this should simply be the conventional ABCD matrix of the 2X2 formalism. (A rigorous proof can be found in [1], as the transition from monochromatic wave to a group is not trivial though it is intuitive). For a time invariant system, $f_{in} = f_{out}$ for every possible case, so the last row has to be $(0, 0, 0, 1)$. From the same argument the third column should be $(0, 0, 1, 0)^T$, because no other component is time dependent, except from t itself. All other remaining components of the 4X4 matrix, represented by the letters E - I, are the additional degrees of freedom caused by the extended formalism.

II. VARIOUS CASES FROM THE ORIGINAL ARTICLE

A. Case I

For the first article case we simulated the multiple prism system used to obtain positive group velocities. the system as described in the article looks as seen in fig(1) :

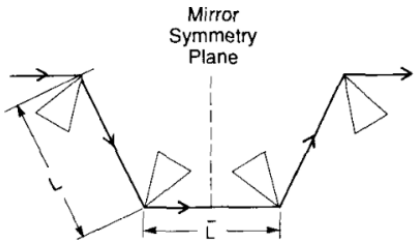

FIG. 1. multiple prism system used to obtain positive group velocities (taken from [1])

The first prism is given by :

$$\begin{bmatrix} M & 0 & 0 & 0 \\ 0 & 1/M & 0 & D \\ MD/\lambda_0 & 0 & 1 & 0 \\ 0 & 0 & 0 & 1 \end{bmatrix} \tag{5}$$

and the second one :

$$\begin{bmatrix} 1/M & 0 & 0 & 0 \\ 0 & M & 0 & -MD \\ -D/\lambda_0 & 0 & 1 & 0 \\ 0 & 0 & 0 & 1 \end{bmatrix} \tag{6}$$

and from the symmetry of the system it is obvious that the next prisms will just be a reflection of the first two. using The aforementioned matrices and free space propagation matrices in between each prism, we obtain the final matrix of the system to be :

$$\begin{bmatrix} 1 & \overline{L} + 2L/M^2 & 0 & 0 \\ 0 & 1 & 0 & 0 \\ 0 & 0 & 1 & -2D^2L/\lambda_0 \\ 0 & 0 & 0 & 1 \end{bmatrix} \tag{7}$$

as seen in [1], using the python script that we wrote that simulates the cases in the article, we got the figure below (fig (2)):

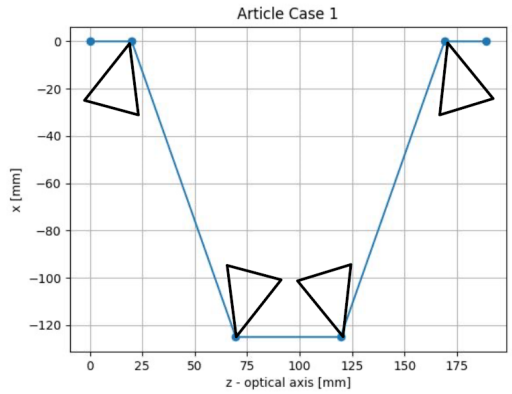

FIG. 2. multiple prism system used to obtain positive group velocities as obtained by our simulation

As can be seen this image matches the one in the article. the final matrix of this system is in the format of the dispersive slab format, (can be seen in Fig (12) in the appendix) which means that this configuration of prisms has the same effect as a dispersive slab.

B. Case II

For the second case given in the article as example, we simulated a system used for short pulse amplification, it can be seen in FIG (3):

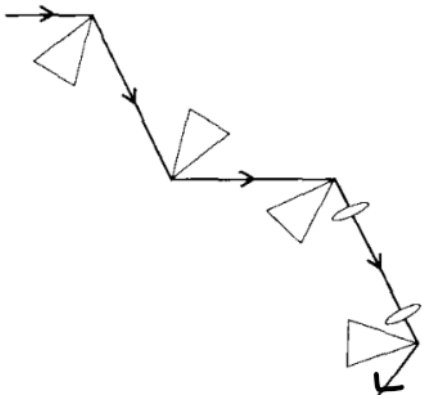

FIG. 3. Short pulse amplification system as seen in [1]

The first three prisms in this case are the same as the ones in Case I, after those matrices we insert a telescope with magnification of -1 and then another prism. The telescope is built using the matrices of two lenses, for each one the matrix is given by:

$$\begin{bmatrix} 1 & 0 & 0 & 0 \\ -1/f & 1 & 0 & 0 \\ 0 & 0 & 1 & 0 \\ 0 & 0 & 0 & 1 \end{bmatrix} \tag{8}$$

so the final matrix of this system is given by:

$$\begin{bmatrix} -1 & \overline{L} & 0 & 0 \\ 0 & -1 & 0 & 0 \\ 0 & 0 & -1 & 0 \\ 0 & 0 & 0 & -1 \end{bmatrix} \tag{9}$$

Using our python code we obtained this figure by simulating the system (fig(4)):

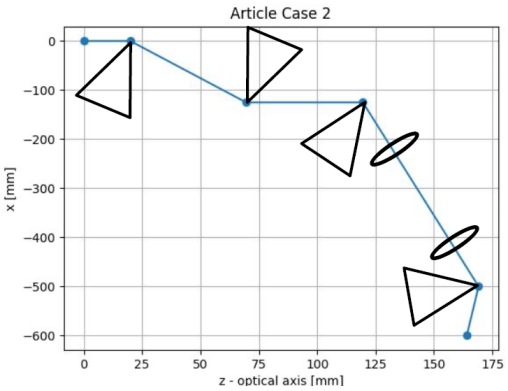

FIG. 4. Short pulse amplification system as obtained by our simulation

The plot indeed looks like the one in the article, and the effect of this system is turning the beam upside down and propagating it backwards.

C. Case III

For the third article example we simulated a general prism beam expander, that can be seen in FIG (5)

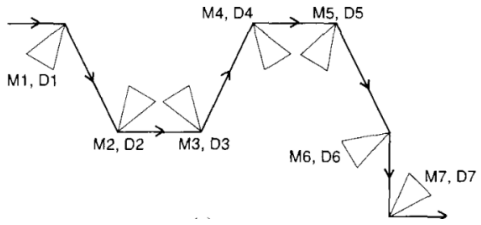

FIG. 5. General prism beam expander as seen in [1]

By looking at the general expression for a prism matrix, such as written in (5), we obtain the final matrix for a beam expander system of k prisms :

$$\begin{bmatrix} \prod_{l=1}^{k} M_l & 0 & 0 & 0 \\ 0 & \frac{1}{\prod_{l=1}^{k} M_l} & 0 & \sum_{l=1}^{k} D_l / \prod_{m=l+1}^{k} M_m \\ \frac{1}{\lambda_0} \sum_{l=1}^{k} D_l \prod_{m=1}^{l} M_m & 0 & 1 & 0 \\ 0 & 0 & 0 & 1 \end{bmatrix} \quad (10)$$

In the numerical simulation we built a configuration like the one presented in fig (5), by using prisms matrices similar to the prisms in case number 1. We simulated a ray which passes the system, as shown in Fig (6):

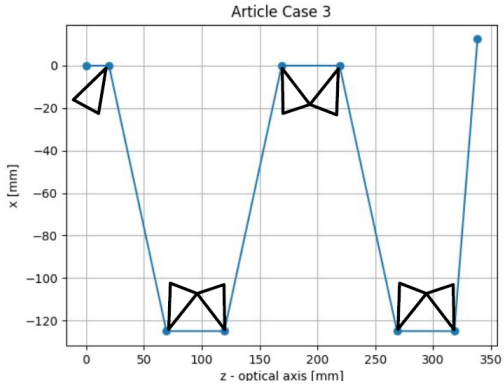

FIG. 6. General prism beam expander as obtained by our simulation

Notice that for different values of M_i and D_i the configuration will look slightly different. For that reason, there is a somewhat of a variance between our plot and the figure given in the article. (For the third case the relation between the different prisms parameters is not mentioned, and lengths in the system is not discussed at much detail as to the extant given in the first two cases).

III. PULSE SHAPER

For this part we examined the configuration of a grating based pulse shaper. The system consists of two diffraction gratings placed on both ends of a 4f lens system. In the Fourier plane of the 4f system, which is placed exactly in the middle between the two lenses (assuming they have the same focal length, which is the case we used in our simulation), an amplitude mask, such as an SLM could be placed, controlling the waveform of the beam which exits the system.

In our simulation, we focused on the simple case where a binary-shaped aperature is placed at the Fourier plane, such that light can only be blocked or pass through it. We entered a polychromatic spacio-temporal rectangular pulse into the system. First, we plotted the case without any amplitude mask (figure (7)), which allowed us to examine the spacial spread of the initial pulse in the Fourier plane, as well as the spacial separation of different wavelengths. Also note, that in the Fourier plane one can notice the varying density of the rays respectively to the different wavelengths (as can be seen in the appendix, Fig numbers (13)(14)).

Then we simulated several cases with different masks, where we let pass or block only wavelengths of one color, only by changing an apperature's position in the Fourier plane (see figures (8)(9)). Also, we placed a slit apperature (figure (10)).

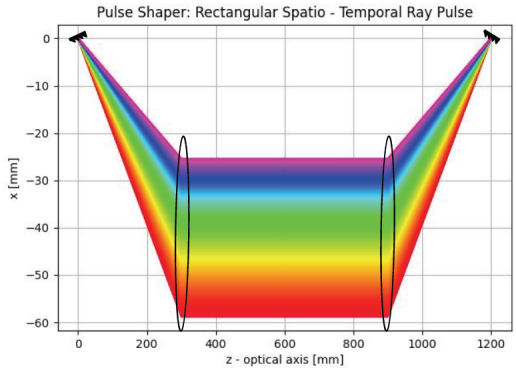

FIG. 7. Pulse shaper without any amplitude mask

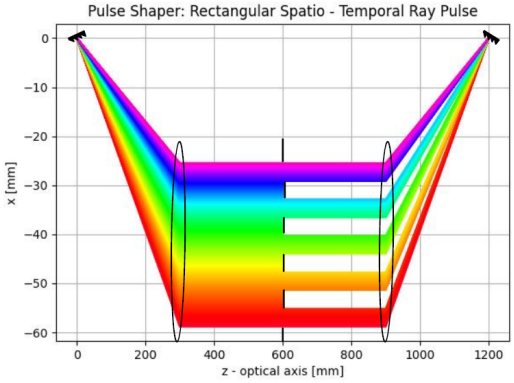

FIG. 10. Pulse shaper with binary slits mask

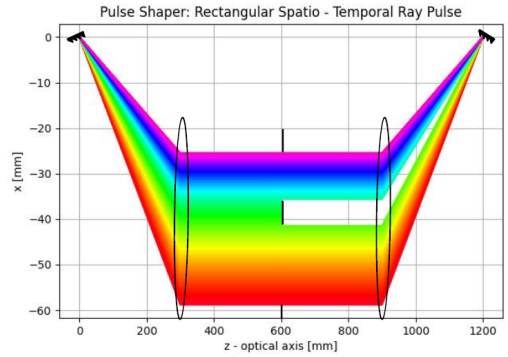

FIG. 8. Pulse shaper with a mask that blockes green light

IV. EXTRA USE CASE: MONOCHROMATOR

As an extra use case, we examine a system of a Czerny–Turner monochromator, which consists of two curved mirrors and a diffraction grating. This optical configuration is used to separate between various wavelengths, e.g. different colors of polychromatic light that enters the system. A narrow slit could be placed at the end, so that only monochromatic light will exit the system, controlled by the slit's position. The configuration seems like it should be simulated using ray beams, but in order to do so we need to take account the frequency component that distinguish different rays. This is a useful case which emphasizes the significance of using an expanded 4X4 formalism, therefore our choice.

In the numerical simulation, we built the system according to the configuration in [5], using the appropriate matrices. Light composed of three different wavelengths enters passes through the system. As seen in (figure (11)), at the exit plane the rays of each wavelength are focused to a different point, as expected.

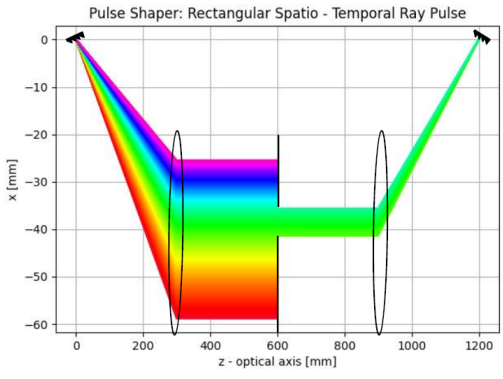

FIG. 9. Pulse shaper with a mask that blocks all the wavelengths besides green

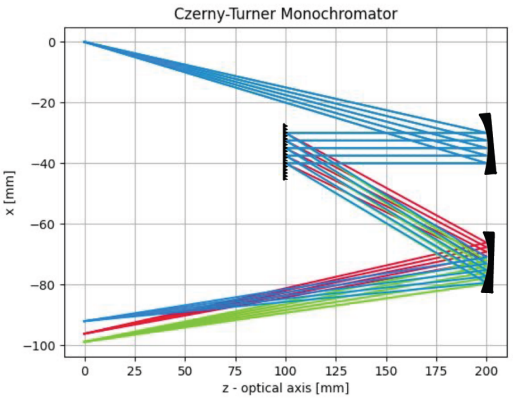

FIG. 11. Simulated monochromator configuration

V. CONCLUSION

In this paper we numerically validated a few of the examples given by Kostenbauder in his work [1], and we also examined the configurations of a grating based pulse shaper and a Czerny - Turner Monochromator, both of this systems are impossible to describe using the standard 2X2 formulation. we were successful in simulating those systems.

VI. REFERENCES

[1] Ray-Pulse Matrices: A Rational Treatment for Dispersive Optical Systems, A. G. KOSTENBAUDER

[2] Laser Beams and Resonators, H. KOGELNIK AND T. LI

[3]O.E. Martinez, "Matrix formalism for pulse compressors"

[4]O.E. Martinez, "Matrix formalism for dispersive laser cavities"

[5]https://en.wikipedia.org/wiki/Monochromator

[6]https://www.rp-photonics.com/pulse$_s hapers.html$

VII. APPENDIX

LENS OR MIRROR	DISPERSIVE SLAB
$\begin{bmatrix} 1 & 0 & 0 & 0 \\ -\frac{1}{f} & 1 & 0 & 0 \\ 0 & 0 & 1 & 0 \\ 0 & 0 & 0 & 1 \end{bmatrix}$ f = focal length	$\begin{bmatrix} 1 & \frac{L}{n} & 0 & 0 \\ 0 & 1 & 0 & 0 \\ 0 & 0 & 1 & -\frac{\partial v_g}{\partial f}\frac{L}{v_g^2} \\ 0 & 0 & 0 & 1 \end{bmatrix}$ L = thickness of slab
LITTROW PRISM	**PRISM**
$\begin{bmatrix} m & 0 & 0 & 0 \\ 0 & \frac{1}{m} & 0 & -\frac{\partial n}{\partial f}\frac{\tan\psi}{m} \\ -\frac{\partial n}{\partial f}\frac{\tan\psi}{\lambda_0} & 0 & 1 & 0 \\ 0 & 0 & 0 & 1 \end{bmatrix}$ ψ = prism apex angle ray enters at normal incidence prism used at tip $m = \sqrt{1-n^2\sin^2\psi}/\cos\psi$	$\begin{bmatrix} m & 0 & 0 & 0 \\ 0 & \frac{1}{m} & 0 & -\frac{\partial n}{\partial f}\tan\psi \\ -\frac{\partial n}{\partial f}\frac{m\tan\psi}{\lambda_0} & 0 & 1 & 0 \\ 0 & 0 & 0 & 1 \end{bmatrix}$ ψ = prism apex angle ray exits at normal incidence prism used at tip $m = \cos\psi/\sqrt{1-n^2\sin^2\psi}$
GRATING	**GENERAL PRISM**
$\begin{bmatrix} -\frac{\sin\phi}{\sin\psi} & 0 & 0 & 0 \\ 0 & -\frac{\sin\psi}{\sin\phi} & 0 & \frac{\cos\phi-\cos\psi}{f_0\sin\phi} \\ \frac{\cos\psi-\cos\phi}{c\sin\psi} & 0 & 1 & 0 \\ 0 & 0 & 0 & 1 \end{bmatrix}$ ψ = incident ray to grating surface angle ϕ = reflected ray to grating surface angle	$A = m_\phi m_\psi$ $B = Lm_\phi/nm_\psi$ $C = 0$ $D = 1/m_\phi m_\psi$ $E = -(\partial n/\partial f)Lm_\phi\tan\psi/n$ $F = -(\partial n/\partial f)(\tan\phi+\tan\psi)/m_\phi$ $G = -(\partial n/\partial f)m_\psi(\tan\phi+\tan\psi)/\lambda_0$ $H = -(\partial n/\partial f)L\tan\phi/m_\psi n\lambda_0$ $I = (\partial n/\partial f)^2 L\tan\phi\tan\psi/n\lambda_0 - (\partial v_g/\partial f)L/v_g^2$ ψ = internal ray to entrance face normal angle ϕ =internal ray to exit face normal angle L = path length in glass $m_\phi = \sqrt{1-n^2\sin^2\phi}/\cos\phi$ $m_\psi = \cos\psi/\sqrt{1-n^2\sin^2\psi}$

FIG. 12. The diffrent 4x4 matrices as given by [1]

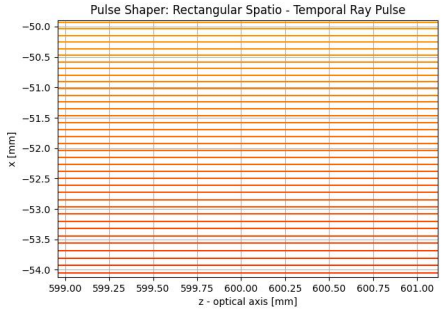

FIG. 14. A zoomed in view of the light beam density from FIg 7 lower end of the spectrum

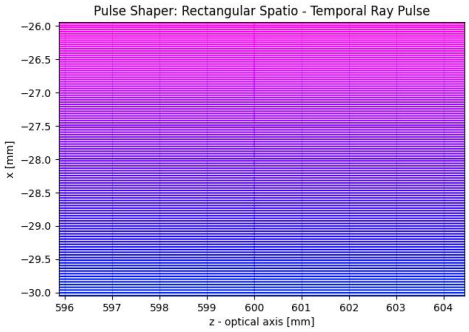

FIG. 13. A zoomed in view of the light beam density from FIg 7 upper end of the spectrum